On the electrochemical behavior of formamidine disulfide on gold electrodes in acid media

William Cheuquepán, José Manuel Orts, Antonio Rodes

PII: S1572-6657(16)30002-9
DOI: doi: 10.1016/j.jelechem.2016.01.002
Reference: JEAC 2443

To appear in: *Journal of Electroanalytical Chemistry*

Received date: 6 November 2015
Revised date: 29 December 2015
Accepted date: 4 January 2016

Please cite this article as: William Cheuquepán, José Manuel Orts, Antonio Rodes, On the electrochemical behavior of formamidine disulfide on gold electrodes in acid media, *Journal of Electroanalytical Chemistry* (2016), doi: 10.1016/j.jelechem.2016.01.002

On the Electrochemical Behavior of Formamidine Disulfide on Gold Electrodes in Acid Media.

William Cheuquepán, José Manuel Orts, Antonio Rodes*
Departamento de Química Física e Instituto Universitario de Electroquímica
Universidad de Alicante, Apartado 99, E-03080 Alicante (Spain)

*Corresponding autor: JM.Orts@ua.es
Tel: +34 965909814
Fax: +34 965909814

ABSTRACT

The adsorption and reactivity of formamidine disulfide (FDS) was studied at gold single crystal and thin film electrodes in perchloric acid solutions and the results of cyclic voltammetry and in situ infrared spectroscopy (SNIFTIR and ATR-SEIRAS) experiments compared with those previously obtained with thiourea (TU). In addition, optimized geometries and theoretical harmonic vibrational frequencies were obtained for adsorbed FDS, TU and thioureate from plane-wave DFT calculations using periodic surface models. These results were compared in the case of TU and thioureate to those previously obtained with a model Au cluster surface with (111) orientation. In the case of FDS, weak adsorption takes place with the S-S bond essentially parallel to the metal surface. No specific bands for adsorbed FDS can be identified in the experimental ATR-SEIRA spectra. These latter spectra suggest that adsorbed thioureate species are spontaneously formed upon dissociative adsorption of FDS when dosing this molecule at open circuit. Some of the adsorbed thioureate species undergo reductive protonation giving rise to a mixed adlayer formed by adsorbed thioureate and thiourea in a surface process which is faster when a controlled potential of 0.70 V is applied. In agreement with the observations reported when dosing TU, the ratio between TU and thioureate adsorbates is found to depend on the electrode potential, being higher for potentials close to the hydrogen evolution limit and decreasing for higher potential values.

Graphical Abstract

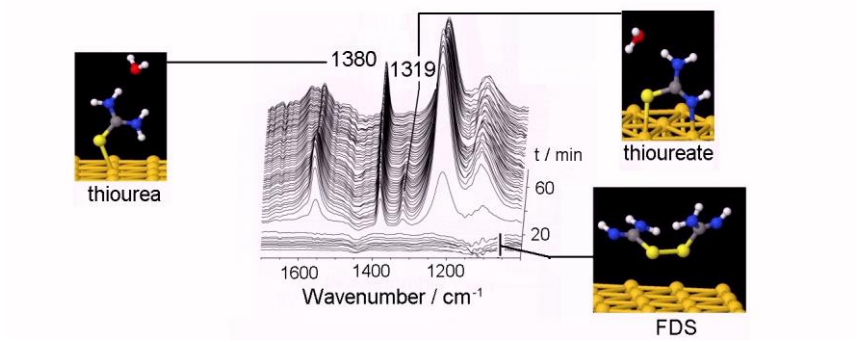

Highlights

- FDS adsorbs weakly on Au with Au-S distances longer than those for TU and thioureate.
- Physisorbed FDS dissociates homolitically to yield adsorbed thioureate.
- Some adsorbed thioureate species are reduced to adsorbed thiourea.
- Dosing conditions influence the rate of formation of adsorbed thiourea.
- The thiourea/thioureate adsorbate ratio depends on the applied potential.

KEYWORDS: formamidine disulfide**,** thiourea, thioureate, gold electrodes, infrared spectroscopy, DFT.

1. Introduction.

Formamidine disulfide (FDS, $(NH_2)(NH)CS\text{-}SC(NH)(NH_2)$) has been reported as the main product of thiourea (TU, NH_2CSNH_2) electrooxidation on gold and platinum electrodes when working at moderate potentials in diluted acidic TU solutions [1-4]

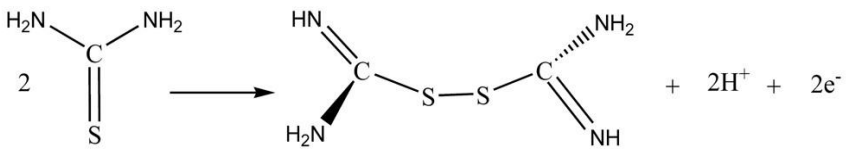

(1)

In the case of gold electrodes, the formation of FDS is paralleled by the oxidative dissolution of gold that takes place at high TU concentrations via the formation of gold-TU complexes [5-7].

The electrochemical behavior of FDS has been studied in connection with that of thiourea [2,8-11]. Several authors reported that the presence of FDS has a strong catalytic effect on the gold dissolution reaction in acidic thiourea solutions [9,11]. The presence of adsorbed TU and FDS species at metal electrodes and their role in the processes described above is a point still open to discussion. As expected from the strong sulfur-metal interaction, a variety of surface techniques has allowed the detection of irreversible adsorbed TU on gold and platinum electrodes in contact with TU-containing solutions [4,6,12-16]. Surface-Enhanced Raman Scattering (SERS) spectroscopy experiments proved the bonding of TU to the metal surface through the sulfur atom [12,13,16-18]. Moreover, both external reflection infrared spectra [6] and surface-enhanced infrared reflection-absorption spectra obtained under attenuated total reflection conditions (ATR-SEIRA) [17] showed bands assigned to the symmetric and asymmetric NCN stretching modes of adsorbed TU. The observation of the latter band implies a significant tilting of the S-C axis with respect to the surface normal. The conclusions on the adsorption geometries of adsorbates (namely, TU and related species) derived from the analysis of spectroscopic data can be supported by theoretical calculations. In this respect, the stability and the interaction with water of TU [19] and thioureate [20], as well as the interaction of TU with anions [21], metallic cations [22], and coordination compounds [23] has been addressed in the past. Regarding the interaction with bulk metals, the only theoretical study dealing with the adsorption of TU, thioureate and FDS is due to Patrito et al [24], who studied these species on cluster models of the Ag(111) surface, using DFT and MP2 methods. In that study, the effects of external electric field and solvation were also addressed. Regarding the interaction of TU and related species with gold surfaces, we are not aware of any theoretical study other than the DFT study carried out by our group [17]. The optimized adsorption geometry for TU on clusters modeling the Au(111) surface was found to correspond to a unidentate configuration for adsorbed TU on top surface sites via the sulfur atom and with the C-S bond tilted by 45º from the normal. This result confirmed the conclusions derived from the observation of the asymmetric NCN band in the in situ infrared spectra [6,17].

Another point of interest that can be addressed by combining spectroelectrochemical data and a theoretical analysis regards the potential-dependent processes undergone by adsorbed thiourea and

the eventual formation of adsorbed FDS. Cyclic voltammograms for gold electrodes in diluted TU solutions are characterized by the presence of surface redox processes in the so-called double layer region of the bare electrode for which different origins have been proposed. Those observed in neutral solutions between -1.10 and 0.40 V SCE were related by Azzaroni et al. [25] to the changes in the in situ STM images as a function of the electrode potential. These authors interpreted the observed ladder-like structures as due to adsorbed FDS, which can be reduced to adsorbed TU or oxidized yielding adsorbed sulfur. On the other hand, a surface redox process at potentials between 0.60 and 0.90 V RHE for gold electrodes in acidic TU-containing solutions has been related to the deprotonation of adsorbed TU to form adsorbed thioureate species [17]. Note that this proposal is connected to previous suggestions regarding the existence of a deprotonation process leading to the formation of adsorbed thioureate on platinum [26], copper [27,28] and gold [29] electrodes that would involve the tautomeric form of the TU molecule

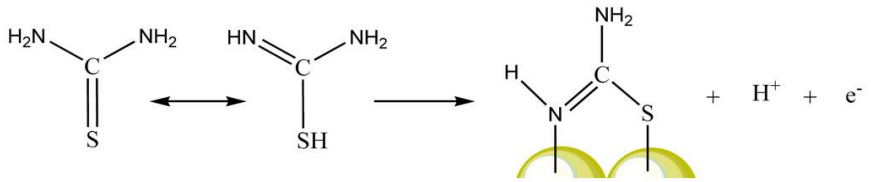

(2)

The presence of adsorbed thioureate at gold electrodes has been inferred from the observation of potential-dependent changes in the characteristic infrared frequencies of the adsorbate formed in TU-containing solutions [17]. Namely, a new band around 1550 cm^{-1} appearing in the ATR-SEIRA spectra collected in water solutions was assigned, according to DFT calculations, to the asymmetric NCN stretching of adsorbed thioureate species. None of the theoretical calculations with adsorbed TU yielded vibrational frequencies near this value. The same holds for the observed band at ca. 1322 cm^{-1} in the spectra collected in D_2O solutions that can only be ascribed to the symmetric NCN stretching of adsorbed deuterated thioureate. The observation of both symmetric and asymmetric NCN bands can be related to the optimized adsorption geometry derived from the DFT calculations for adsorbed thioureate [17], which implies bidentate bridge bonding via both the S atom and the N atom of the NH group, with the molecular plane perpendicular to the surface and the C-S bond tilted around 60-70º from the surface normal. Finally, the presence in the spectra collected in D_2O solutions of a band at 1380 cm^{-1} characteristic of deuterated TU, at potentials as high as 0.90 V indicates the presence of significant amounts of coadsorbed TU coexisting with thioureate at this potential.

This paper reports a spectroelectrochemical study of FDS adsorption on gold electrodes. The nature of the adsorbed species formed from diluted FDS solutions is investigated in potential and FDS concentration range selected in order to minimize further FDS oxidation and/or the dissolution of the gold electrode via the formation of TU complexes, these processes being out of the scope of this paper. Voltammetric and spectroscopic data obtained in acidic media with Au(111) and Au(100) single crystal electrodes are compared to those for gold thin-film electrodes and with the previously published results for adsorbed TU. As in previous studies recently published by our group [17,30-37], infrared spectroscopy is used to gain molecular level information on the bonding of these adsorbed molecules. The reported experiments combine the use of single-crystal electrode surfaces (in external reflection infrared experiments) and gold thin film electrodes (for ATR-SEIRAS). The use of ordered gold thin films with a preferential (111) orientation as electrodes in the so-called Kretschmann's configuration (ATR-SEIRAS experiments) allows comparisons with the behavior of gold single crystal electrodes while keeping the enhanced surface sensitivity. This characteristic behavior facilitates the detection of adsorbates at low coverages (thus allowing the use of low FDS concentrations for which solution or surface dissolution processes are not significant) as well as the study of interactions between adsorbed species and interfacial water molecules [38,39]. In order to better support the assignment of experimental vibrational frequencies, DFT calculations will be used for obtaining optimized adsorbate geometries and theoretical harmonic vibrational frequencies of adsorbed FDS, TU and thioureate species. We have selected in this case a slab model with periodic boundary conditions for modeling the metal surface, in order to allow for the calculation of the FDS adsorbate, that would require too big a cluster, which makes the cluster calculation extremely costly. Moreover, the slab model with nonlocalized basis sets provides a much better description of the metallic properties of the solid. In order to allow for comparisons within the same computational framework, we have also carried out slab calculations with adsorbed thiourea and thioureate species which give results that are basically similar to those previously obtained from cluster models [17] and are presented as supplementary materials.

2. Model and Computational Details

All the DFT calculations in this paper were carried out using the Vienna Ab-initio Simulation Package (VASP, v-4.6) [40-43], using the GGA exchange-correlation functional of Perdew, Burke and Ernzerhof (PBE) [44,45], which is known to be a good compromise for describing both metal surfaces and molecular systems, as well as adsorbates. As a basis set we used a system of Projector

Augmented Waves (PAW) [46,47] with a cutoff energy of 400 eV. The selection of k-points for sampling the Brillouin zone was done with the automatic Monkhorst-Pack method [48], using a centered (3x3x1) set. For smearing, we chose the second order Methfessel-Paxton method [49]with a sigma value of 0.2 eV.

The simulation cell used for modelling the Au(111) surface consisted of four layers of gold atoms with the (4x4) structure (16 atoms each), with a vacuum region of more than 1.2 nm, that ensures that no significant coupling exist between periodic replica in the Z-direction. The cell dimensions amounted to 1.1808 nm x 1.1808 nm x 2.1693 nm, that are in all the three axis sufficiently greater than the longest distance between two atoms in FDS (0.691 nm). This rules out the possibility of hydrogen bonding between FDS adsorbates in neighbouring replica that could arise because of the periodic boundary conditions. In order to keep modest the computational costs, and as our main interest in these calculations is obtaining the optimized geometries and harmonic vibrational frequencies of the adsorbate in the range accesible in our experiments, in the optimization procedure we have only allowed the molecular adsorbate to relax (starting from a number of different starting geometries), while the metal nuclei are kept at fixed positions, with a lattice constant of 0.41748 nm (nearest-neighbour distances of 0.29520 nm). This value was obtained from a series of bulk energy calculations with different lattice constant, and fitting to the Murnaghan equation of state. This value coincides with the calculated values reported by other authors for the PBE functional, and compares well with the experimental value of 0.40789 nm [50]. We also carried out some test calculations allowing the relaxation of one metal layer, with minor differences in the adsorbates' optimized geometries and calculated frequencies.

The convergence criteria were: 10^{-5} eV for the electronic step, and 0.2 eV/nm for the forces on the atoms in the geometry optimization. All calculations were carried out with a total zero charge. Frequency calculations were done with a value of POTIM=0.02. The assignment of the vibrational normal modes to the calculated frequencies has been done on the basis of the visualization of the vibrational motions using Molden [51] and Jmol [52].

As discussed in our previous paper [17], the inclusion of some explicit water molecules in the model is necessary in order to obtain calculated frequencies as close as possible to the experimental ones. This is a consequence of the effect of hydrogen bonding on the force constants of the combination normal modes. The calculation of theoretical frequencies has been repeated for the fully-deuterated species, as all the hydrogen atoms in the considered molecules are bonded to nitrogen atoms and are thus exchangeable with the deuterium atoms of the D_2O solvent. All values of theoretical

frequencies are given unscaled and expressed in cm^{-1}. In general, the calculated frequencies obtained by these calculation methods usually agree well with the experimental ones (with discrepancies below a few percent).

3. Experimental Section

Concentrated perchloric acid (Merck Suprapur®), FDS (dihydrochloride, Merck, >97%) and ultrapure water (18.2 MΩ·cm, Elga Vivendi) were used to prepare the working solutions, which were deaerated with Ar (N50, Air Liquide). Solutions in deuterated water were prepared with deuterium oxide (99.9 atom %D, Aldrich).

All the voltammetric and in situ infrared experiments were performed in glass cells using a gold wire as the counter electrode and a reversible hydrogen electrode (RHE) as the reference electrode. Gold single crystals prepared from a high purity gold wire (99,9998% Alfa-Aesar) following Clavilier's method [53,54] were used as working electrodes in the electrochemical (ca. 2.0 mm in diameter) and in situ external reflection infrared spectroscopy experiments (diameter around 4.5 mm). Prior to each experiment, these electrodes were heated in a gas-oxygen flame, cooled down in air and protected with a droplet of ultrapure water [54-56]. In the internal reflection infrared spectroscopy experiments, the working electrode was a 25 nm-thick gold thin film thermally evaporated on a silicon prism. Film deposition was carried out in the vacuum chamber of a PVD75 (Kurt J. Lesker Ltd.) coating system at a base pressure around 10^{-6} Torr. A quartz crystal microbalance was used to monitor both the deposition rate, which was fixed at 0.006 nm s^{-1}, and the thin-film thickness. After assembling the spectroelectrochemical cell, the gold film was electrochemically annealed by cycling the electrode potential in a 0.1 M $HClO_4$ + 10 mM CH_3COONa solution which was latter replaced by an acetate-free perchloric acid solution [57].

The spectroelectrochemical cells used in this work are equipped with a prismatic window (Si or CaF_2, for the internal and external reflection experiments, respectively) beveled at 60° [58,59]. In situ infrared experiments were carried out using a Nexus 8700 (Thermo Scientific) spectrometer equipped with a MCT-A detector. All the spectra were obtained with a resolution of 8 cm^{-1} and are presented in absorbance units (a.u.). Positive-going and negative-going bands correspond, respectively, to gain or loss of species for the sample spectrum with respect to the reference spectrum. Sets of 100 (ATR-SEIRAS) or 200 (external reflection experiments) interferograms were collected at different sample potentials and referred to a proper reference single beam spectrum. In

the case of the ATR-SEIRA spectra this single beam spectrum was obtained before dosing FDS in the 0.1 M $HClO_4$ solution.

4. Results and discussion.

4.1. DFT calculation of optimized adsorption geometries and harmonic infrared frequencies for adsorbed FDS.

As stated above, periodic DFT calculations have been carried out for obtaining optimized geometries of adsorbed FDS species and the corresponding theoretical harmonic vibrational frequencies, which can be used as a guide for the assignment of the experimental vibrational frequencies reported in this work. Besides, calculated adsorbate geometries can be used to confirm conclusions on the surface orientation derived from the application of the surface selection rule for infrared absorption at metal surfaces [60,61]. The latter precludes the observation of vibrational modes giving rise to changes in the dynamic dipole with a zero component in the direction normal to the metal surface. Figure 1 shows the optimized geometry of FDS on the 4-layer slab Au(111)-(4x4) model surface. As it is clearly seen, the molecule adsorbs with its disulfide bond axis oriented nearly parallel to the metal surface. The sulfur atoms are slightly displaced from top positions, and the S-S bond is slightly misaligned with respect to the dense surface metal rows. Both halves of the molecule have their molecular planes forming angles around 45º with respect to the surface. One half is slightly closer to the surface than the other. Comparison of the geometric details (bond lengths, angles and dihedrals, given in Table 1) with those obtained with FDS in the gas phase (not given) indicates that the effect of adsorption on the FDS geometry are relatively small. This suggests that the adsorbate-surface interaction is weak (and does not involve significant changes in its electronic structure). Besides, the two S-Au distances, that amount to 0.326 and 0.339 nm, are both significantly longer than the values found after geometry optimization for TU (0.261 nm) and thioureate (0.246 nm) (see supplementary information), which are characteristic of strong sulfur-metal chemical bonds. It can then be concluded that the optimized geometry obtained for adsorbed FDS corresponds to a physisorbed FDS species.

Figure 1

Table 1

Table 2

Table 2 shows a group of selected theoretical vibrational frequencies of adsorbed FDS which can be compared to the corresponding values in the gas phase (given in parentheses). As in the case of bond length and angles reported in Table 1, the good correlation between frequency values for the adsorbed and the free FDS molecule indicates a weak molecule-surface interaction. Due to the presence of functional groups in the FDS molecule that are similar to those in TU and thioureate, one could expect similar infrared absorption bands as those calculated for these species (see ref. [17] and/or supplementary information). However, some differences can be remarked from the calculated values. The most distinctive feature of the theoretical FDS spectrum is the presence of vibrations due to the asymmetric NCN stretch (with minor contributions from the scissoring of the NH_2 group) around 1680 cm^{-1} in water and around 1650 cm^{-1} in deuterium oxide. These frequencies are substantially higher than in the case of TU and thioureate, and are related to an increased bonding order in the NCN moiety (due to the existence of a C=N double bond, which is not present in the other two adsorbates). However, with the optimized geometry shown in Figure 1, the dynamic dipole of the asymmetric NCN stretch would be parallel to the metal surface and thus infrared inactive both in external reflection [60] and in ATR-SEIRA [61] experiments due to the corresponding surface selection rule. On the other hand, the band with contribution from the symmetric NCN stretch appears in the calculated spectra at ca. 1270 cm^{-1} for FDS-H and 1084 cm^{-1} for the deuterated isotopomer. This latter band would be infrared active but it must be kept in mind that the significant deviation of the molecular planes (around 45º) with respect to the surface normal would make difficult the observation of such adsorbate, as the z-component of the transition dipole moments would be significantly lower as compared to the case where these molecular planes are perpendicular to the surface.

4.2. Spectroelectrochemical experiments in FDS-containing solutions.

4.2.1. Gold single crystal electrodes.

Figure 2 shows cyclic voltammograms for the Au(111) and Au(100) electrodes in FDS-containing perchloric acid solutions. At low FDS concentrations (equal to or below 0.05 mM) a redox process between 0.40 and 0.70 V (similar to that found in TU solutions, see Figure S1A) is observed for both electrodes. Increasing the FDS concentration gives rise to the observation of additional reduction processes at potentials below 0.3-0.4 V whose current densities increase for increasing FDS

concentrations. The voltammetric profiles become similar to those previously reported by several authors [2,8-11], with prevalent diffusion-control characteristics and ascribed to the reduction of FDS to TU. Differences between the first and second cycle (stationary) when contact is made at 0.70 V in the 1 mM FDS solution can be rationalized on the basis of the formation of adsorbed TU-related species at this potential, including those involved in the dissolution of the gold electrode surface (vide infra). The anodic counterpart in the stationary voltammograms recorded for high enough FDS concentrations may involve the re-oxidation of TU either to FDS or TU-gold complexes [2,8-11].

Figure 2

Figure 3

External reflection experiments with gold single crystals have been limited to relatively concentrated solutions (above 1 mM) in order to increase the chances to detect absorption bands. Under these conditions one can expect the observation of bands corresponding to species involved in the solution reactions or to the onset of gold dissolution via the formation of gold-thiourea complexes. Thus, and even if the study of the solution and dissolution processes mentioned above processes are out of the scope of this work, the obtained spectra have to be analyzed in connection with the voltammetric behaviour described in Figure 2 for high FDS concentrations,

As in most of the in-situ external reflection infrared experiments reported for TU, deuterium oxide was used as the solvent in order to avoid interferences from the bending bands of water [6,17]. As a similar spectroelectrochemical behavior has been observed for Au(111) and Au(100) electrodes in the FDS-containing solution, we will describe in the following only the infrared spectra obtained with Au(111). Figure 3 shows a set of potential-difference external reflection spectra collected in a 10 mM FDS solution with a Au(111) electrode using p-polarised light. The reference spectrum was collected at 0.70 V in the FDS-containing solution just after the immersion of the flame-annealed electrode at this potential. Then, the electrode potential was stepped to decreasing potentials down to 0.10 V and the corresponding sample spectra were collected.

Negative-going bands appearing around 1635, 1569, 1396 and 1326 cm^{-1} correspond to species present at the reference potential (either at the electrode surface or in the thin solution layer between the electrode and the infrared window) which are consumed when decreasing the electrode potential. As the band at 1635 cm^{-1} is also observed with s-polarized light (see bottom spectrum), it can be

stated, according to the surface selection rule for external reflection infrared experiments [60], that this feature corresponds to a dissolved species. The bands at 1635 and 1396 cm^{-1} were also observed in the infrared spectra collected during the oxidation of TU and were ascribed to dissolved FDS (asymmetric and symmetric NCN stretching modes, respectively) [6,17]. The band at 1396 cm^{-1} can be hardly appreciated in the spectrum reported in Figure 3 for s-polarization due to a poor signal-to-noise ratio and some overlapping with the positive-going feature at around 1384 cm^{-1}. On the other hand, the positive-going band at around 1384 cm^{-1}, which corresponds to species formed at the sample potential and is observed with both p- and s-polarized light (in this latter case with a poor signal-to-noise ratio), can be assigned to dissolved TU molecules formed upon FDS reduction [6]. The spectra in figure 3 show that the bands at 1569 cm^{-1} and 1320 cm^{-1} are observed with p-polarized but not with s-polarized light. As a consequence of the surface selection rule [60], this is the expected behavior of adsorbate vibrations giving rise to a change of the dynamic dipole of the species with a non-zero component normal to the electrode surface. The band at 1569 cm^{-1} fits well with that assigned to the asymmetric NCN stretching of the gold-thiourea complex (Au(I)-TU_2) being formed during TU oxidation [6,17]. In the experiments reported in Figure 2, this species would be already formed and accumulated at the electrode surface in the presence of TU at the immersion potential. Regarding the band at 1326 cm^{-1}, its frequency fits with that of the typical feature for adsorbed deuterated thioureate detected in deuterium oxide solutions [17]. As it will be shown below, the observation of this feature in the external reflection experiment is consistent with the ATR-SEIRA spectra obtained when dosing FDS at 0.70 V on a gold thin film electrode.

4.2.2. Gold thin film electrodes.

As a first conclusion from the experiments described in the previous section, it can be stated that no bands that could be ascribed solely to adsorbed FDS can be observed in the external reflection infrared spectra. Interferences from solution species associated to the use of a relatively high FDS concentration in the external reflection experiments, the effect of gold oxidation under these conditions and the adsorption of FDS in a flat configuration (see above) could be at the origin of this behavior. A much better signal-to-noise ratio and high surface specificity (allowing the use of very diluted FDS solutions) are expected in the ATR-SEIRAS experiments carried out with Au(111)-25 nm electrodes, thus avoiding some of the problems commented above. These experiments also allow the study of the time-dependent behavior of FDS adsorption after dosing. Figure 4 shows a set of time-dependent ATR-SEIRA spectra collected after the addition of 0.05 mM FDS at 0.70 V in a 0.1

M perchloric acid test solution prepared in water. These spectra are referred to the single beam spectrum collected at the same electrode potential in the supporting electrolyte before the addition of FDS. Several positive-going bands appear in the resulting absorbance spectra obtained under these conditions with their intensities increasing with time after dosing. In addition to the strong broad band centered around 3500 cm^{-1} related mainly to the O-H stretching of interphasial water molecules [38,39,62], some additional features are observed in the frequency region between 1700 and 1200 cm^{-1}, which are similar to those observed in experiments carried out in TU-containing solutions (see figure S1 in the supplementary material). Namely, main absorption bands are observed at ca. 1650 and 1420 cm^{-1}. As previously discussed on the basis of DFT calculations using cluster models [17] and also confirmed by new calculations using periodical slab models (see tables S2 and S3 in the supplementary material), these features (assigned to NH_2 scissoring and symmetric NCN stretch modes, respectively) are common for adsorbed TU and thioureate anions. Besides, a small feature is observed around 1554 cm^{-1} whose intensity first increases for short times after dosing and then decreases (see Figure 4 and the corresponding plot in Figure 5). This band can be assigned to the asymmetric NCN stretching (see reference 17 and table S3) of adsorbed thioureate that could be formed upon homolytic dissociative adsorption of FDS:

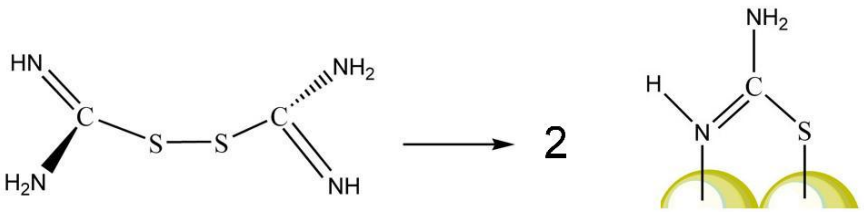

(3)

In order to confirm this assignment, the same experiment (dosing FDS at 0.70 V) was repeated in a deuterium oxide solution. The spectra obtained are shown as an inset in Figure 4, which shows the time-dependent behavior of the absorption bands appearing after dosing. A shift of the observed bands towards lower wavenumbers, similar to that previously reported for TU [17] (see also figure S1), is related to the deuteration of the adsorbates formed upon FDS dosing. In this way, the band at ca. 1650 cm^{-1} (in water) appears as a split feature between 1500 and 1600 cm^{-1}. Also, a couple of bands can be observed at 1380 and 1320 cm^{-1}, with related band intensities after dosing. As shown in figure 5, the intensity of the band at 1380 cm^{-1}, that has been ascribed to adsorbed deuterated TU (see reference 17 and table S2), increases in a steep way for short dosing times and later with a lower slope. On the contrary, a feature at 1320 cm^{-1} that can be assigned to adsorbed deuterated thioureate (see reference 17 and table S3), appears at short times after dosing and fades out very slowly with

time. This behavior, that suggests the formation of a mixture of adsorbed TU and thioureate at the dosing potential (with TU prevailing with increasing time after dosing), is consistent with the time-dependent behavior of the intensity of band at 1550 cm^{-1} for adsorbed thioureate in Figure 4, which decreases with time after dosing (see also the corresponding plot in figure 5) . The absence of the corresponding band at 1500 cm^{-1} for the asymmetric NCN stretching of adsorbed TU in the spectra collected in water (figure 4) can be due to its low intensity (see the spectra in Figure S1B).

Figure 4

The time-dependent formation of adsorbed TU to the detriment of the adsorbed thioureate species coming from the dissociative adsorption of FDS can be related to a reductive protonation of adsorbed thioureate

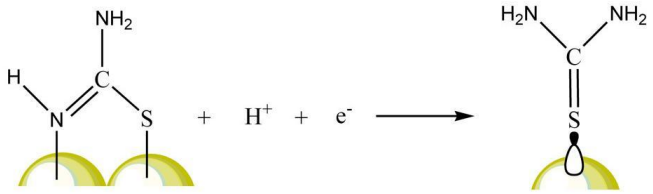

(4)

The kinetics of this transformation can be potential-dependent and is expected to be slower at open circuit conditions, since direct charge transfer across the metal/solution interface would not be possible. We have repeated the FDS dosing experiments under these conditions. ATR-SEIRA spectra in water and D_2O solutions are shown in Figure 6 and the corresponding band intensities are plotted in Figure 5 (filled symbols). The spectra collected in water show that the band at 1550 cm^{-1} decreases at a lower rate after dosing when compared with the behavior reported in Figure 7 when dosing at 0.70 V. Consequently, the growth with time of the intensity of the band at 1380 cm^{-1} for adsorbed TU proceeds more slowly than under close circuit conditions (compare close and open circles in Figure 5). The existence of some kind of local cell mechanism (with some species being oxidized in order to afford the electrons needed for reducing adsorbed thioureate) can be invoked for explaining the formation of adsorbed TU under open circuit conditions.

Figure 5

Figure 6

As in the case of the external reflection experiments, the analysis of the spectra shown in Figures 4 and 6 confirms the absence of infrared absorption bands related to adsorbed FDS since all the observed features can be ascribed to adsorbed TU or thioureate species. However, the spectra in figures 4 and 6 show, both under open and closed circuit conditions, that there is a significant and reproducible delay (of several minutes) between the adsorption time and the beginning of the observation of positive adsorbate bands. In the same time lapse, however, some negative-going bands can be distinguished. These latter features are attributable to interphasial water molecules, which would be displaced from the metal surface as the formation of some adsorbed species. We can tentatively propose that this species is physically adsorbed FDS. This weakly adsorbed FDS would act in turn as a precursor leading to the formation of adsorbed thioureate via a homolytic dissociation process. This interpretation of the experimental facts is compatible with the adsorption geometry depicted in Figure 1. As discussed above, the orientation of adsorbed FDS with respect to the surface would make be very difficult the detection of the characteristic FDS bands for the asymmetric and asymmetric NCN stretchings since their corresponding dynamic dipole moments would be, respectively, parallel or nearly parallel to the metal surface. In this respect, it has to be pointed out that no feature is observed around 1270 cm^{-1} in the spectra obtained in water solutions that could be related to the symmetric NCN band of adsorbed FDS-H. Positive-going bands are observed in the spectra reported in figures 4 and 6 only when significant amounts of adsorbed thioureate and TU (this latter species being formed upon reductive protonation of adsorbed TU) are formed from physisorbed FDS.

Figure 7

A last piece of information regarding the nature of the adsorbates formed upon FDS dosing is related to the effect of the electrode potential on the stationary ratio between adsorbed TU and thioureate adsorbates, which can be derived from the relative intensities of the bands at 1500/1550 cm^{-1} (water) or 1380/1320 cm^{-1} (deuterium oxide). The cyclic voltammogram obtained with the Au(111)-25 nm electrode in the 0.05 mM FDS solution (Figure 7A) is similar to that discussed above for TU (Figure S1 A), with a redox surface process at potentials above 0.40 V. Figures 7 B and C show two sets of ATR-SEIRA spectra obtained after FDS dosing and reaching a stationary spectrum at 0.70 V in experiments carried out in water and in deuterium oxide solutions, respectively. The first set was collected by decreasing the electrode potential from 0.70 V down to 0.10 V (spectra a) while the second set was collected subsequently by increasing the electrode potential from 0.10 to 1.0 V

(spectra b). A first observation when inspecting spectra a is the increase of the band at ca. 1643 cm^{-1} after stepping the electrode potential from 0.60 to 0.30 V. Since this band appears both in the spectra of adsorbed TU and thioureate (see supplementary material), this behavior can be related to an increase of the amounts of FDS being dissociated to form thioureate (equation 3) and which is reduced to adsorbed TU upon reduction (equation 4). Note that the intensity of the band at ca. 1643 cm^{-1} is almost constant in the spectra collected at 0.10 V and also in the spectra collected when stepping the electrode potential up to 1.0 V (spectra b), thus suggesting that the sum of TU and thioureate coverages has reached a nearly constant value. The second observation derived from the spectra in Figure 7 is related to the relative intensity of the specific features for adsorbed TU and thioureate. In water, the band at 1550 cm^{-1} for adsorbed thioureate in the spectrum collected at 0.60 V is replaced at 0.10 V by the feature at 1500 cm^{-1}associated to adsorbed TU. In deuterium oxide solutions, the feature at 1380 cm^{-1} that can be assigned to deuterated TU and is also observed at 0.70 V, increases when the electrode potential is lowered, whereas the band at 1320 cm^{-1} that can be ascribed to deuterated thioureate is hardly detectable in the spectrum collected at 0.10 V. This behavior is similar to that observed in the TU-containing solutions (see figures S1B and C) [17]. As under these latter conditions, the transformation of adsorbed thioureate into adsorbed TU can be reverted if the sample electrode is increased up to 1.0 V (reappearance of the bands at 1557 and 1320 cm^{-1} in water and deuterium oxide, respectively). On the basis of these observations, we can pose the question of the eventual formation of adsorbed FDS as the result of the potential-driven oxidation of adsorbed TU. Once again, it has to be pointed out that no spectroscopic evidence can be found in the spectra reported in Figure 7 regarding presence of adsorbed FDS irrespective of the electrode potential. Namely, no band can be detected around 1270 cm^{-1} in the spectra obtained in water solutions (figure 7B) assignable to the symmetric NCN stretch of adsorbed FDS-H. This fact, together with the good correlation between the frequencies of the adsorbate bands which are specific of the ATR-SEIRA spectra collected at high potentials (namely, the features at 1550 cm^{-1} in water and 1320 cm^{-1} deuterium oxide solution) and those calculated for adsorbed thioureate, would suggest the absence of adsorbed FDS formed upon oxidation of adsorbed TU. However, the presence of some amount of adsorbed FDS with an adsorption geometry as that derived from DFT calculations can not be completely discarded due to the low value of the dynamic dipole of infrared active FDS bands in the direction normal to the metal surface. The same arguments can be used to confirm that our previous interpretation of the surface redox process in the TU-containing solutions as related to the existence of a surface equilibrium between adsorbed TU and thioureate species (not FDS) [17] is essentially correct.

5. Conclusions.

Cyclic voltammetry and in-situ FTIR spectroscopy (both under external reflection and attenuated total reflection conditions) have been used to study experimentally the spectroelectrochemical behavior of formamidine disulfide (FDS) on gold electrodes (single crystals and nanostructured thin layers with preferential (111) orientation). FDS is found to undergo below 0.5 V RHE a reduction process leading to thiourea as the final product, in agreement with previous results of other groups. This process shows peak currents for FDS concentrations above 1mM that indicate limitations due to mass transport from the solution. The consumption of dissolved FDS and the concomitant production of dissolved TU are detected by in situ external reflection infrared measurements. In these experiments, the observation of an absorption band at 1569 cm^{-1} is tentatively interpreted as due to the formation of an adsorbed gold-thiourea complex at the immersion potential of 0.70 V.

The formation of adsorbates in diluted (0.05 mM) FDS solutions have been also studied in ATR-SEIRAS experiments and the nature of the adsorbates analyzed with the help of the calculated harmonic frequencies corresponding to the optimized adsorption geometries derived from plane-wave DFT calculations carried out for adsorbed FDS, adsorbed TU and adsorbed thioureate. Periodic DFT calculations using PAW basis set and the PBE functional have essentially confirmed the adsorption geometries of TU and thioureate previously obtained from B3LYP/6-31+G*,LANLDZ using cluster models. TU bonds to the gold surface in unidentate configuration through the sulfur atom, with the CS bond significantly tilted from the surface normal. Thioureate bonds to the gold surface in a bidentate configuration, using the sulfur and the nitrogen atom with lower hydrogen coordination. Both adsorbates have their molecular planes perpendicular to the metal surface. In the case of FDS, the periodic calculations indicate that it adsorbs weakly, with the sulfur-sulfur bond parallel to the metal surface and Au-S distances significantly longer than those found in the case of adsorbed TU and thioureate. DFT calculations of vibrational frequencies of adsorbed thiourea and thioureate have yielded values that agree well with the experimental ones (within errors lower than 4-5%). We have verified again the importance of including in the model for calculations some explicit water molecules in order to allow the formation of hydrogen bonds with the species of interest, this allowing a better estimation of the frequencies of the normal modes.

Time-resolved ATR-SEIRAS experiments have put in evidence the formation of adsorbates other than FDS when dosing this molecule at low concentrations (0.05 mM). It has been observed, both under open and closed circuit conditions, that there is a significant and reproducible delay (of several minutes) between the dosing time and the beginning of the observation of positive adsorbate bands. These bands can not be ascribed specifically to adsorbed FDS. According to our DFT calculations, undissociated adsorbed FDS has the S-S axis almost parallel to the gold surface with the two S-C axis forming angles around 45º with respect to the surface. In any case, with this optimized adsorption geometry the variation of the dynamic dipole for the asymmetric NCN stretching (with an expected frequency around 1660 cm^{-1} both for deuterated and non deuterated FDS) would be parallel to the electrode surface. Regarding the symmetric NCN stretching mode, the latter would have a dynamic dipole with a small non zero component normal to the gold surface. Note this mode would show a strong isotopic shift (from ca. 1270 to ca. 1084 cm^{-1}) when comparing non-deuterated and deuterated species that is not observed when replacing water by deuterium oxide as the solvent in spectroelectrochemical experiments. On the other hand, the ATR-SEIRA spectra can be rationalized by assuming the formation of a mixture of adsorbed thioureate and TU since all the observed bands can be ascribed to one of these species. Thus, it can be concluded that physically adsorbed FDS acts in turn as a precursor leading to the formation of strongly adsorbed thioureate via a homolitic dissociative adsorption process. These adsorbed thioureate species can be further reduced into adsorbed TU, in a surface redox process involving one electron and proton per adspecies. This process has been observed even at open circuit, probably involving some local cell mechanism, and is found to increase its rate upon circuit closure. The relative ratio TU/thioureate, as estimated from the integration of their respective characteristic bands, suggests that this process is a potential-controlled surface equilibrium. This confirms the conclusions reached in a previous paper where the observed redox process in TU-containing solutions was ascribed to the transformation between adsorbed TU and adsorbed thioureate.

Acknowledgements

The authors acknowledge the financement by Ministerio de Economía y Competitividad (project CTQ2013-44083-P) and the University of Alicante. William Cheuquepán is grateful for the award of a F.P.I. grant associated to project CTQ2009-13142. Professor Juan M. Feliu is gratefully acknowledged for kindly providing the gold single crystals used in this work.

Figure captions

Figure 1. Top (left) and lateral (right) views of the optimized geometry of FDS adsorbed on a model Au(111)-(4x4) surface.

Figure 2. Cyclic voltammograms obtained for Au(111) and Au(100) electrodes recorded in x mM FDS + 0.1 M $HClO_4$ solutions. a) x = 0 ; b) x = 0.01 ; c) x = 0.05 ; d) x = 1. Solid lines correspond to the first voltammetric cycle after immersion at 0.70 V. Curves d2 correspond to to the stationary voltammogram in the 1 mM solution. Sweep rate: 50 $mV \cdot s^{-1}$.

Figure 3. Potential-dependent infrared spectra collected with p- or s-polarized light for a Au(111) electrode in a 10 mM FDS+0.1 M $HClO_4$ solution prepared in D_2O. The reference spectrum was collected at 0.70 V (the immersion potential) in the same solution.

Figure 4. Time-dependent ATR-SEIRA spectra collected at 0.70 V after dosing 0.05 mM FDS in a 0.1 M $HClO_4$ solution. The inset shows spectra collected in a similar experiment carried out with the working solution being prepared in deuterium oxide. The reference spectra were collected at 0.70 V in the FDS-free solution.

Figure 5. Plots of the time-dependent normalized integrated intensities of the typical bands for adsorbed thioureate and TU in FDS dosing experiments carried out in water or in deuterium oxide solutions. Empty and full symbols correspond to dosing at 0.70 V and open circuit, respectively. The intensity of each band is normalized to its maximum value reached at short (TU) or high (thioureate) times after dosing.

Figure 6. Time-dependent ATR-SEIRA spectra collected at open circuit after dosing 0.05 mM FDS in a 0.1 M $HClO_4$ solution. The inset shows spectra collected in a similar experiment carried out with the working solution being prepared in deuterium oxide. The reference spectra were collected at 0.70 V in the FDS-free solution.

Figure 7. A) Cyclic voltammetry of a Au(111)-25nm surface in contact with a 0.05 mM FDS in 0.1 M perchloric acid solution. B) Typical potential-dependent ATR-SEIRAS spectra in H_2O obtained at different sample potentials. C) Typical potential-dependent ATR-SEIRAS spectra in D_2O obtained at different sample potentials. The spectra in panels B and C were collected after dosing FDS at 0.70 V and collecting a stationary spectrum in experiments similar to those reported in Figure 5 for water (B) and D_2O (C) solutions. The reference spectrum was collected at 0.70 V in the corresponding perchloric acid solution before FDS dosing. Arrows indicate the direction of the potential excursions after FDS dosing.

References

1. M. Yan, K. Liu, and Z. Jiang, "*Electrochemical oxidation of thiourea studied by use of in situ FTIR spectroscopy*", J. Electroanal. Chem., 408 (1996) 225-229.
2. A. E. Bolzan, I. B. Wakenge, R. C. Salvarezza, and A. J. Arvia, "*Electrochemical response of thiourea and formamidine disulphide on polycrystalline platinum in aqueous 0.5 M sulphuric acid*", J. Electroanal. Chem., 475 (1999) 181-189.
3. A. E. Bolzan, P. L. Schilardi, R. C. V. Piatti, T. Iwasita, A. Cuesta, C. Gutierrez, and A. J. Arvia, "*Comparative voltammetric and FTIRRAS study on the electro-oxidation of thiourea and methyl-thioureas on platinum in aqueous acid solutions*", J. Electroanal. Chem., 571 (2004) 59-72.
4. G. Garcia, J. L. Rodriguez, G. I. Lacconi, and E. Pastor, "*Adsorption and oxidation pathways of thiourea at polycrystalline platinum electrodes*", J. Electroanal. Chem., 588 (2006) 169-178.
5. A. E. Bolzan, T. Iwasita, and A. J. Arvia, "*In situ FTIRRAS study of the electro-oxidation reactions of thiourea and gold in aqueous acid solutions*", J. Electroanal. Chem., 554-555 (2003) 49-60.
6. G. Garcia, J. L. Rodriguez, G. I. Lacconi, and E. Pastor, "*Spectroscopic investigation of the adsorption and oxidation of thiourea on polycrystalline Au and Au(111) in acidic media*", Langmuir, 20 (2004) 8773-8780.
7. M. Tian and B. E. Conway, "*Effects of thiourea on anodic dissolution of Au and surface oxidation behaviour in aqueous $HClO_4$ studied by means of an EQCN*", J. Appl. Electrochem., 34 (2004) 533-543.
8. H. Zhang, I. M. Ritchie, and S. R. La Brooy, "*Electrochemical oxidation of gold and thiourea in acidic thiourea solutions*", J. Electrochem. Soc., 148 (2001) D146-D153.
9. X. Yang, M. S. Moats, and J. D. Miller, "*The interaction of thiourea and formamidine disulfide in the dissolution of gold in sulfuric acid solutions*", Miner. Eng., 23 (2010) 698-704.
10. A. E. Bolzan, R. C. V. Piatti, and A. J. Arvia, "*Electrochemical processes at gold|thiourea-containing aqueous acid solution interfaces*", J. Electroanal. Chem., 552 (2003) 19-34.
11. J. Li and J. D. Miller, "*Reaction kinetics for gold dissolution in acid thiourea solution using formamidine disulfide as oxidant*", Hydrometallurgy, 63 (2002) 215-223.
12. G. K. Parker and G. A. HOPE, "*Spectroelectrochemical investigations of gold leaching in thiourea media*", Miner. Eng., 21 (2008) 489-500.
13. J. Z. Zheng, B. Ren, D. Y. Wu, and Z. Q. Tian, "*Thiourea adsorption on a Pt surface as detected by electrochemical methods and surface-enhanced Raman spectroscopy*", J. Electroanal. Chem., 574 (2005) 285-289.
14. G. Deschenes and E. Ghali, "*Leaching of gold from a chalcopyrite concentrate by thiourea*", Hydrometallurgy, 20 (1988) 179-202.
15. Z. D. Stankovic and M. Vukovic, "*The influence of thiourea on kinetic parameters on the cathodic and anodic reaction at different metals in H_2SO_4 solution*", Electrochim. Acta, 41 (1996) 2529-2535.
16. R. Holze and S. Schomaker, "*New results on the electrosorption of urea and thiourea on gold electrodes*", Electrochim. Acta, 35 (1990) 613-620.
17. W. Cheuquepan, J. M. Perez, J. M. Orts, and A. Rodes, "*Spectroelectrochemical and DFT Study of Thiourea Adsorption on Gold Electrodes in Acid Media*", J. Phys. Chem. C, 118 (2014) 19070-19084.
18. P. Gao, M. L. Patterson, M. A. Tadayyoni, and M. J. Weaver, "*Gold as a ubiquitous*

substrate for intense surface-enhanced Raman scattering", Langmuir, 1 (1985) 173-176.
19. W. Zhou, Y. Wen, and L. Qiu, "*Structure and stability of thiourea with water, DFT and MP2 calculations*", J. Mol. Struct. : THEOCHEM, 730 (2005) 133-141.
20. W. Yang, W. Zhou, and K. Peng, "*Structure and stability of thioureate anions with water, DFT calculations*", J. Mol. Struct. : THEOCHEM, 858 (2008) 101-106.
21. D. A. Jose, A. Singh, A. Das, and B. Ganguly, "*A density functional study towards the preferential binding of anions to urea and thiourea*", Tetrahedron Lett., 48 (2007) 3695-3698.
22. G. M. S. El-Bahy, B. A. E-Sayed, and A. A. Shabana, "*Vibrational and electronic studies on some metal thiourea complexes.*", Vibrational Spectroscopy, 31 (2003) 101-107.
23. S. Banerjee, P. S. Sengupta, and A. K. Mukherjee, "*A detailed theoretical study of the interaction of thiourea with cis-diaqua(ethylenediamine) platinum (II).*", J. Mol. Struct. : THEOCHEM, 913 (2009) 97-106.
24. E. M. Patrito, F. P. Cometto, and P. Paredes-Olivera, "*Quantum mechanical investigation of thiourea adsorption on Ag(111) considering electric field and solvent effects*", J. Phys. Chem. B, 108 (2004) 15755-15769.
25. O. Azzaroni, G. Andreasen, B. Blum, R. C. Salvarezza, and A. J. Arvia, "*Scanning tunneling microscopy studies of the electrochemical reactivity of thiourea on Au(111) electrodes*", J. Phys. Chem. B, 104 (2000) 1395-1398.
26. A. E. Bolzan, R. C. V. Piatti, R. C. Salvarezza, and A. J. Arvia, "*Electrochemical study of thiourea and substituted thiourea adsorbates on polycrystalline platinum electrodes in aqueous sulfuric acid*", J. Appl. Electrochem., 32 (2002) 611-620.
27. V. Brunetti, B. Blum, R. C. Salvarezza, A. J. Arvia, P. L. Schilardi, A. Cuesta, J. E. Gayone, and G. Zampieri, "*Scanning Tunneling Microscopy, Fourier Transform Infrared Reflection-Absorption Spectroscopy, and X-ray Photoelectron Spectroscopy of thiourea adsorption from aqueous solutions on silver (111)*", J. Phys. Chem. B, 106 (2002) 9831-9838.
28. V. Brunetti, B. Blum, R. C. Salvarezza, and A. J. Arvia, "*Comparative molecular resolution STM imaging of thiourea, ethylthiourea, and sulfur self-assembled adlayer structures on silver (111)*", Langmuir, 19 (2003) 5336-5343.
29. A. E. Bolzan and A. J. Arvia, "*Adsorption and electro-oxidation of N-alkyl and N,N'-dialkyl thioureas on gold electrodes in acid solutions. A combined FTIRRAS and voltammetry study*", J. Solid State Electrochem., 12 (2008) 529-543.
30. A. P. Sandoval, J. M. Orts, A. Rodes, and J. M. Feliu, "*Adsorption of glycine on Au(hkl) and gold thin film electrodes: an in situ spectroelectrochemical study*", J. Phys. Chem. C, 115 (2011) 16439-16450.
31. *Diffraction and Spectroscopic Methods in Electrochemistry*", Wiley-VCH, Weinheim, 2006.
32. A. P. Sandoval, J. M. Orts, A. Rodes, and J. M. Feliu, *"DFT and in situ infrared studies on adsorption and oxidation of glycine, L-alanine, and L-serine on gold electrodes"*, in Vibrational Spectroscopy at Electrified Interfaces, Wieckowski, A., Korzeniewski, C., and Braunschweig, Bjorn (Eds.)2013, 241-265.
33. A. P. Sandoval, J. M. Orts, A. Rodes, and J. M. Feliu, "*A comparative study of the adsorption and oxidation of L-alanine and L-serine on Au(100), Au(111) and gold thin film electrodes in acid media*", Electrochim. Acta, 89 (2013) 72-83.
34. A. Berna, J. M. Delgado, J. M. Orts, A. Rodes, and J. M. Feliu, "*Spectroelectrochemical study of the adsorption of acetate anions at gold single crystal and thin-film electrodes*", Electrochim. Acta, 53 (2008) 2309-2321.

35. J. M. Delgado, R. Blanco, J. M. Orts, J. M. Pérez, and A. Rodes, "*DFT and in-situ spectroelectrochemical study of the adsorption of fluoroacetate anions at gold electrodes*", J. Phys. Chem. C, 113 (2009) 989-1000.
36. J. M. Delgado, R. Blanco, J. M. Orts, J. M. Pérez, and A. Rodes, "*Glycolate adsorption at gold and platinum electrodes: A theoretical and in situ spectroelectrochemical study*", Electrochim. Acta, 55 (2010) 2055-2064.
37. J. M. Delgado, R. Blanco, J. M. Perez, J. M. Orts, and A. Rodes, "*Theoretical and spectroelectrochemical studies on the adsorption and oxidation of glyoxylate and hydrated glyoxylate anions at gold electrodes*", J. Phys. Chem. C, 114 (2010) 12554-12564.
38. M. Osawa, "*Dynamic processes in electrochemical reactions studied by surface-enhanced infrared absorption spectroscopy (SEIRAS)*", Bull. Chem. Soc. Jpn., 70 (1997) 2861-2880.
39. T. Wandlowski, K. Ataka, S. Pronkin, and D. Diesing, "*Surface enhanced infrared spectroscopy-Au(1 1 1-20 nm)/sulphuric acid - new aspects and challenges*", Electrochim. Acta, 49 (2004) 1233-1247.
40. G. Kresse and J. Hafner, "*Ab initio molecular dynamics of liquid metals*", Phys. Rev. B: Condens. Matter, 47 (1993) 558-561.
41. G. Kresse and J. Hafner, "*Ab initio molecular-dynamics simulation of the liquid-metal-amorphous-semiconductor transition in germanium*", Phys. Rev. B: Condens. Matter, 49 (1994) 14251-14269.
42. G. Kresse and J. Furthmueller, "*Efficient iterative schemes for ab initio total-energy calculations using a plane-wave basis set*", Phys. Rev. B: Condens. Matter, 54 (1996) 11169-11186.
43. G. Kresse and J. Furthmuller, "*Efficiency of ab-initio total energy calculations for metals and semiconductors using a plane-wave basis set*", Comput. Mater. Sci., 6 (1996) 15-50.
44. J. P. Perdew, K. Burke, and M. Ernzerhof, "*Generalized gradient approximation made simple*", Phys. Rev. Lett., 77 (1996) 3865-3868.
45. J. P. Perdew, K. Burke, and M. Ernzerhof, "*Generalized gradient approximation made simple. [Erratum to document cited in CA126:51093]*", Phys. Rev. Lett., 78 (1997) 1396.
46. P. E. Bloechl, "*Projector augmented-wave method*", Phys. Rev. B: Condens. Matter, 50 (1994) 17953-17979.
47. G. Kresse and D. Joubert, "*From ultrasoft pseudopotentials to the projector augmented-wave method*", Phys. Rev. B: Condens. Matter Mater. Phys., 59 (1999) 1758-1775.
48. H. J. Monkhorst and J. D. Pack, "*Special points for Brillouin-zone integrations*", Physical Review B-Condensed Matter, 13 (1976) 5188-5192.
49. M. Methfessel and A. T. Paxton, "*High-precision sampling for Brillouin-zone integration in metals*", Phys. Rev. B: Condens. Matter, 40 (1989) 3616-3621.
50. C. Kittel and M. Vollmer, "*Introduction to solid state physics*", Wiley, New York, 5th, 1976.
51. G. Schaftenaar and J. H. Noordik, "*Molden: a pre- and post-processing program for molecular and electronic structures*", J. Comput. -Aided Mol. Des., 14 (2000) 123-134.
52. "*Jmol: an open-source Java viewer for chemical structures in 3D.*", http://www. jmol. org, (2015).
53. J. Clavilier, D. Armand, S.-G. Sun, and M. Petit, "*Electrochemical adsorption behaviour of platinum stepped surfaces in sulphuric acid solutions*", J. Electroanal. Chem., 205 (1986) 267-277.

54. A. Rodes, E. Herrero, J. M. Feliu, and A. Aldaz, "*Structure sensitivity of irreversibly adsorbed tin on gold single-crys tal electrodes in acid media*", J. Chem. Soc. Faraday. Trans., 92 (1996) 3769-3776.
55. D. M. Kolb, "*Reconstruction phenomena at metal-electrolyte interfaces*", Prog. Surf. Sci., 51 (1996) 109-173.
56. A. Hamelin, "*Cyclic voltammetry at gold single-crystal surfaces .1. Behaviour at low index faces*", J. Electroanal. Chem., 407 (1996) 1-11.
57. J. M. Delgado, J. M. Orts, J. M. Pérez, and A. Rodes, "*Sputtered thin-film gold electrodes for in situ ATR-SEIRAS and SERS studies*", J. Electroanal. Chem., 617 (2008) 130-140.
58. A. Rodes, J. M. Pérez, and A. Aldaz, *"Vibrational Spectroscopy"*, in Handbook of Fuel Cells. Fundamentals, Technology and Applications., Vielstich, W., Gasteiger, H. A., and Lamm, A. (Eds.)John Wiley & Sons Ltd., Chichester, 2003, 191-219.
59. J. M. Delgado, J. M. Orts, and A. Rodes, "*ATR-SEIRAS Study of the Adsorption of Acetate Anions at Chemically Deposited Silver Thin Film Electrodes*", Langmuir, 21 (2005) 8809-8816.
60. R. G. Greenler, "*Infrared study of adsorbed molecules on metal surfaces by reflection techniques*", J. Chem. Phys., 44 (1966) 310-315.
61. M. Osawa, K. Ataka, K. Yoshii, and Y. Nishikawa, "*Surface-enhanced Infrared Spectroscopy : the origin of the absorption enchancement and band selection rule in the infrared spectra of molecules adsorbed on fine metal particles*", Appl. Spectrosc., 47 (1993) 1497-1502.
62. K. Ataka, T. Yotsuyanagi, and M. Osawa, "*Potential-dependent reorientation of water molecules at an electrode/e lectrolyte interface studied by surface-enhanced infrared absorption spectroscopy*", J. Phys. Chem., 100 (1996) 10664-10672.

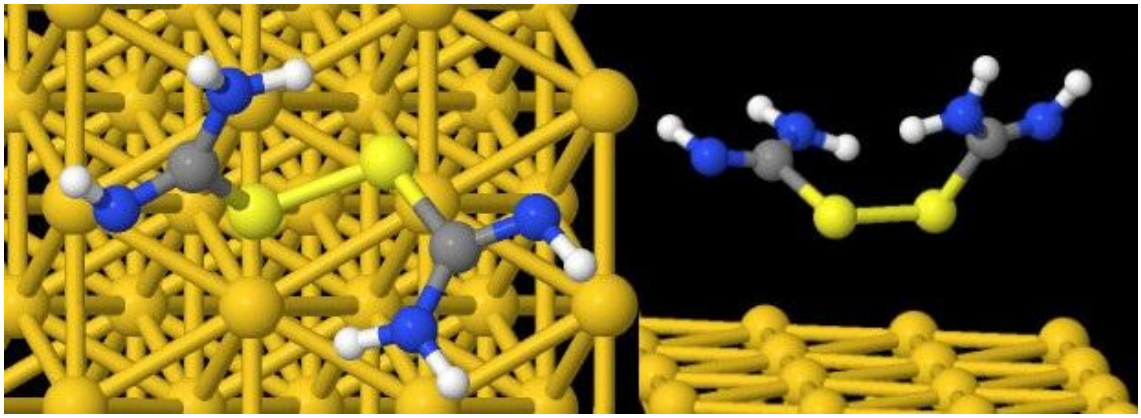

Fig. 1

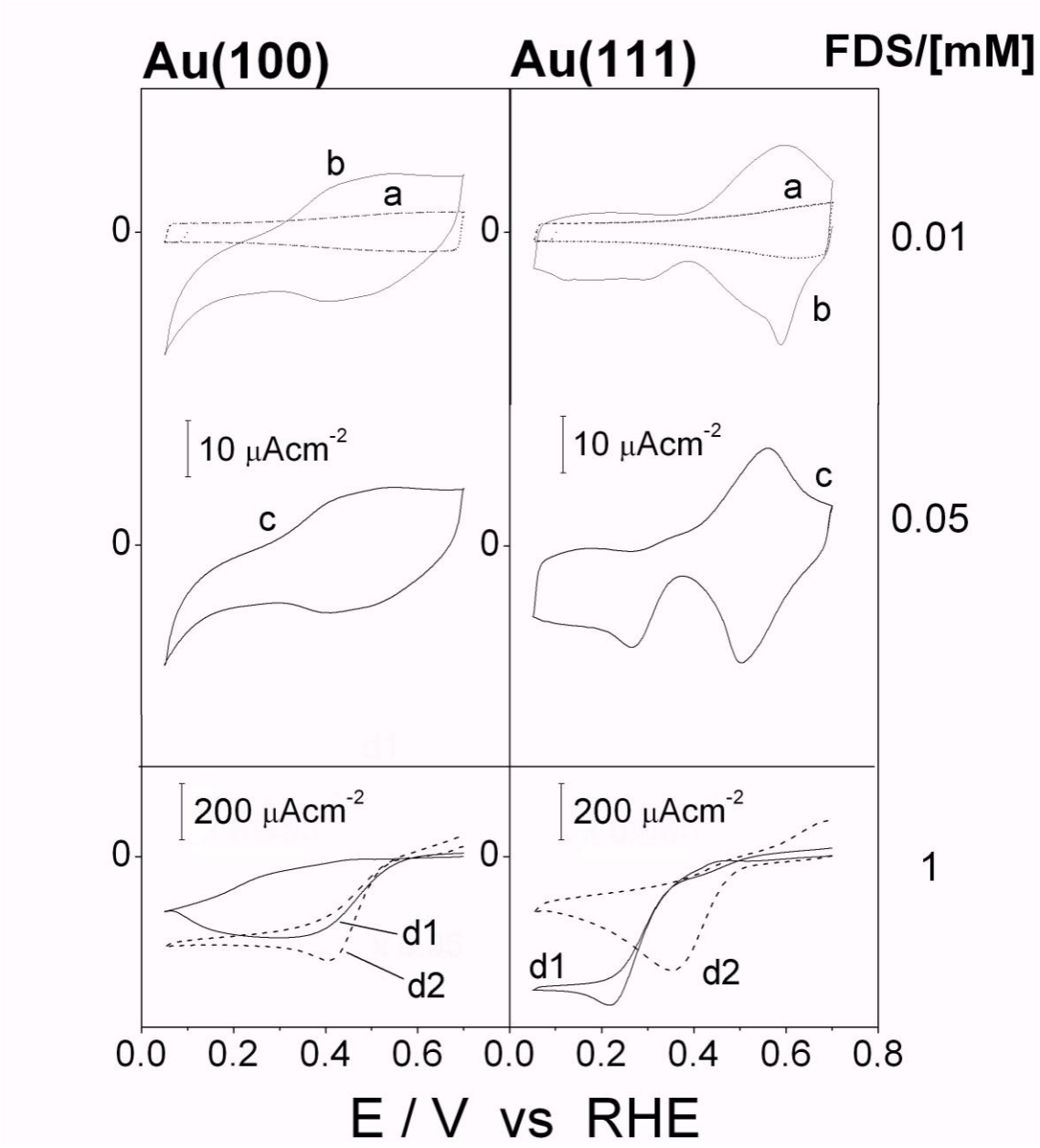
Au(100)
Au(111)
FDS/[mM]
b
a
a
b
0
0
0.01
10 μAcm-2
10 μAcm-2
c
c
0
0
0.05
200 μAcm-2
200 μAcm-2
0
0
1
d1
d2
d1
d2
0.0
0.2
0.4
0.6
0.0
0.2
0.4
0.6
0.8
E / V vs RHE

Fig. 2

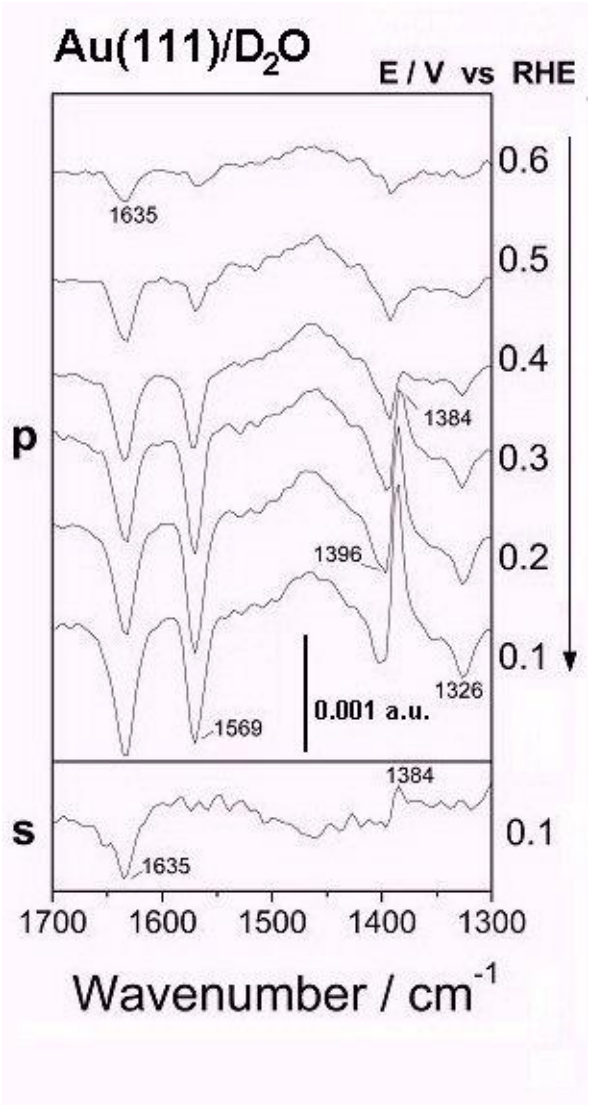
Au(111)/D2O
E / V vs RHE
0.6
0.5
0.4
0.3
0.2
0.1
p
s
1635
1384
1396
1326
1569
0.001 a.u.
1700
1600
1500
1400
1300
Wavenumber / cm-1

Fig. 3

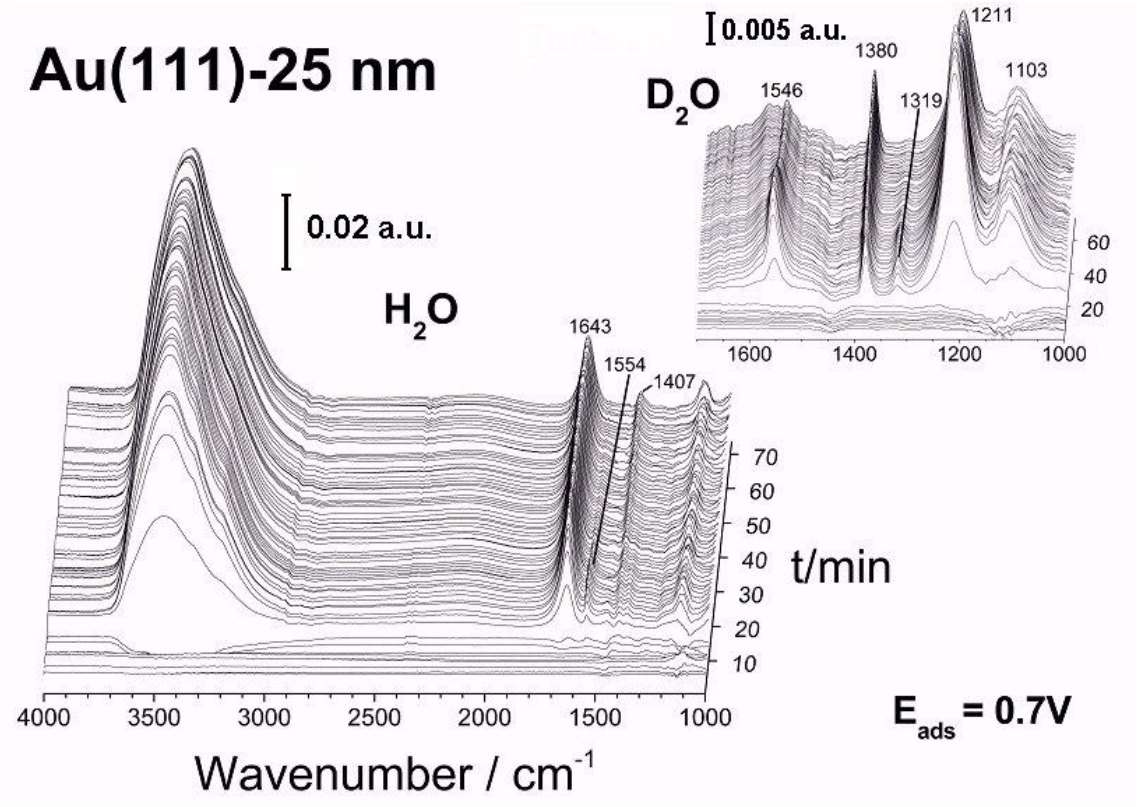
Au(111)-25 nm
0.005 a.u.
D2O
1211
1380
1103
1546
1319
60
40
20
1600
1400
1200
1000
0.02 a.u.
H2O
1643
1554
1407
70
60
50
40
30
20
10
t/min
4000
3500
3000
2500
2000
1500
1000
Eads = 0.7V
Wavenumber / cm-1

Fig. 4

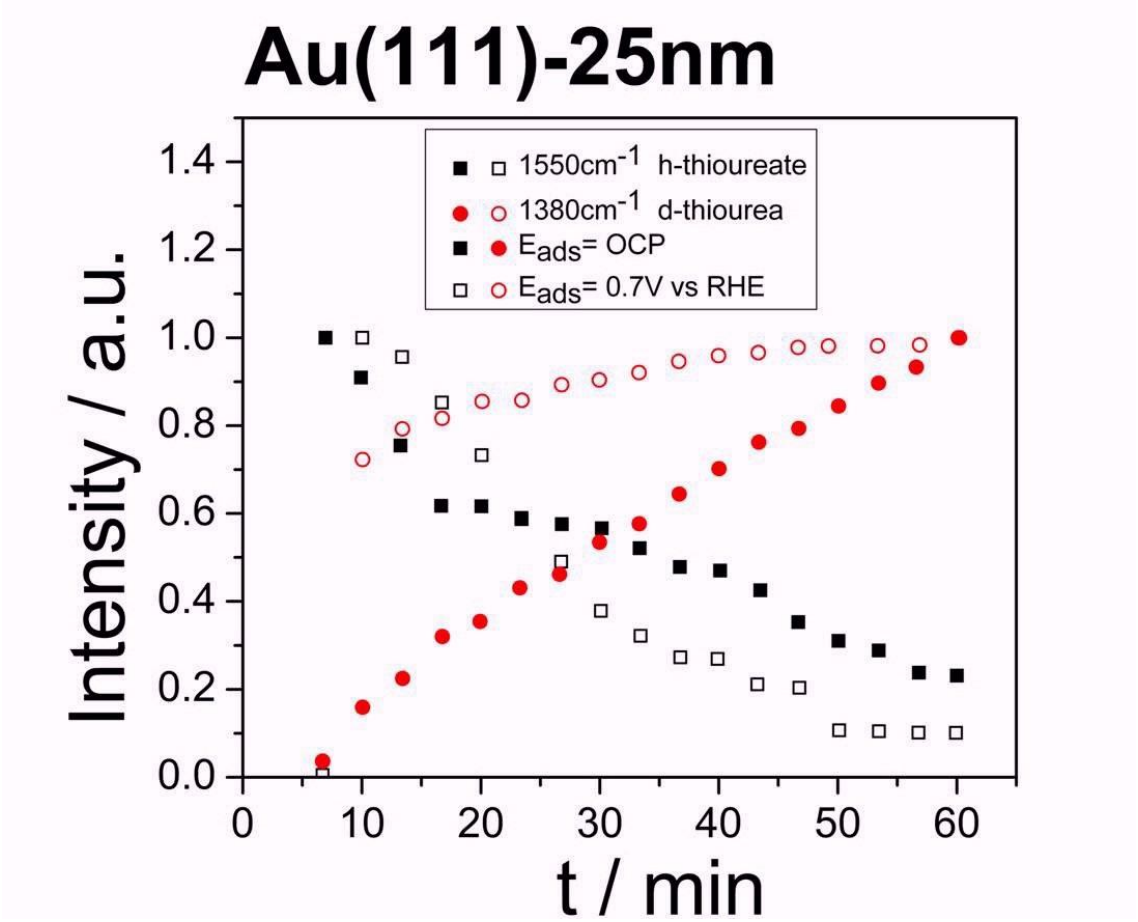
Au(111)-25nm
1550cm-1 h-thioureate
1380cm-1 d-thiourea
Eads= OCP
Eads= 0.7V vs RHE
Intensity / a.u.
t / min
0.0
0.2
0.4
0.6
0.8
1.0
1.2
1.4
0
10
20
30
40
50
60

Fig. 5

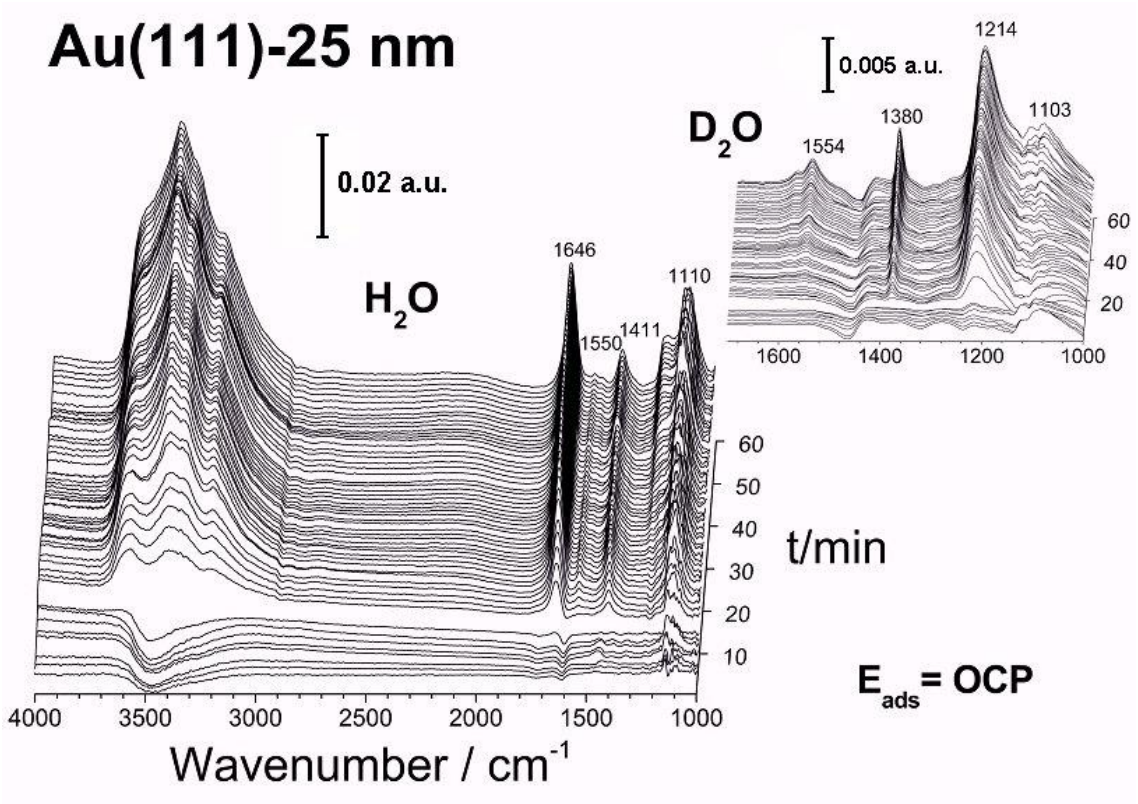
Au(111)-25 nm
0.02 a.u.
H2O
1646
1550
1411
1110
60
50
40
30
20
10
t/min
4000
3500
3000
2500
2000
1500
1000
Wavenumber / cm-1
Eads = OCP
0.005 a.u.
D2O
1554
1380
1214
1103
60
40
20
1600
1400
1200
1000

Fig. 6

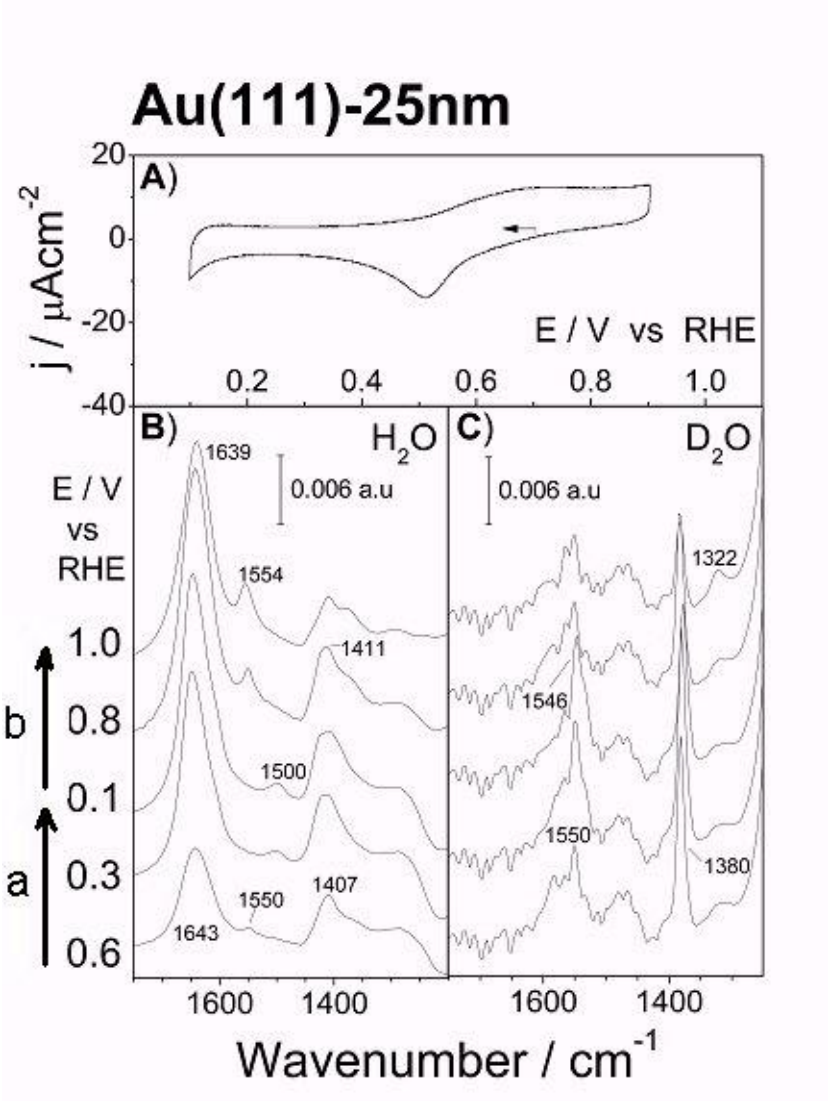
Au(111)-25nm
A)
j / μAcm-2
E / V vs RHE
B)
H2O
C)
D2O
0.006 a.u
E / V vs RHE
1639
1554
1411
1500
1407
1550
1643
1322
1546
1550
1380
b
a
1.0
0.8
0.1
0.3
0.6
Wavenumber / cm-1

Fig. 7

Table 1. Selected bond distances and angles of the optimized geometry of adsorbed FDS on Au(111)-(4x4) surface. All distances in nm, all angles in degrees. Discrepancies in bond length values between the molecular part close to the surface and that far from the surface are below 1 pm unless otherwise stated. Discrepancies in angles are below 1º.

S-Au = 0.326 S-Au = 0.339	S-S = 0.205	ϕ C-S-S-C = 93.7
N-H = 0.103	C-NH = 0.128	Θ CNH = 114
N-H(2) = 0.102	C-NH2 = 0.136	Θ HNH = 118
C-S = 0.182	Θ CSS = 107	Θ NCN = 132.5

Table 2. Selected theoretical vibrational frequencies of FDS (and the fully-deuterated FDS) adsorbed on the Au(111)-(4x4) model surface and in gas phase (in parentheses).

FDS-H	Assignment	FDS-D	Assignment
1680 (1634)	Asym st NCN + sciss NH_2, ip	1654 (1609)	Asym st NCN + sciss ND_2, ip
1676 (1625)	Asym st NCN + sciss NH_2, oop	1650 (1598)	Asym st NCN + sciss ND_2, oop
1547 (1581)	Sciss NH_2 + sym st NCN, ip	1287 (1256)	Sym st NCN + rock ND_2 + bend CND, ip
1541 (1578)	Sciss NH_2 + sym st NCN, oop	1270 (1249)	Sym st NCN + rock ND_2 + bend CND, oop
1277 (1298)	Sym st NCN + bend CNH + rock NH_2, ip	1084 (1128)	Sciss ND_2 + sym st NCN, ip
1260 (1296)	Sym st NCN + bend CNH + rock NH_2, oop	1083 (1128)	Sciss ND_2 + sym st NCN, oop

Ip = in phase vibrations; Oop = out of phase vibrations